Aquaculture 584 (2024) 740644

Contents lists available at ScienceDirect

Aquaculture

journal homepage: www.elsevier.com/locate/aquaculture

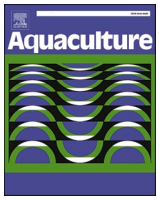

Ecophysiological response of the cupped oyster *Crassostrea gigas* exposed to the green dinoflagellate *Lepidodinium chlorophorum*

Pauline Roux [a,b], José Luis García-Corona [c], Stacy Ragueneau [d,c], Mathilde Schapira [b], Raffaele Siano [e], Fabrice Pernet [c], Isabelle Queau [c], Pascale Malestroit [e], Kevin Tallec [c], Elodie Fleury [c,*]

[a] Nantes Université, Institut des Substances et Organismes de la Mer, ISOMer, UR 2160, F-44000 Nantes, France
[b] Ifremer LITTORAL, Rue de l'Ile d'Yeu 44311, Nantes, France
[c] Univ Brest, CNRS, IRD, Ifremer, UMR 6539, LEMAR, F-29280 Plouzane, France
[d] Aix Marseille Univ, CNRS, Centrale Marseille, M2P2, Equipe Procédés Membranaires (EPM), Marseille, France
[e] Ifremer, DYNECO, F-29280 Plouzané, France

ARTICLE INFO

Keywords:
Harmful algae blooms
Dinoflagellate *Lepidodinium chlorophorum*
Oysters *Crassostrea gigas*
Ecophysiological impairment

ABSTRACT

Green seawater discolorations caused by the marine dinoflagellate *Lepidodinium chlorophorum* are frequently observed during the summer along the southern coast of Brittany, France. Although there is no evidence that L. *chlorophorum* produces toxins, green seawater discolorations are related to mortalities of filter feeding animals. Here, we investigate the ecophysiological response of the Pacific oyster *Crassostrea gigas* exposed to L. *chlorophorum*. Oysters were exposed for 48 h to a low concentration (500 cells mL^{-1}) and a bloom concentration (7500 cells mL^{-1}) of L. *chlorophorum* and compared to controls fed with the haptophyte *Tisochrysis lutea*. The direct consequences of L. *chlorophorum* exposure were assessed through semiquantitative histochemical analysis. Thereafter, a 24 h-recovery phase with a diet based on *T. lutea* was studied using an individual ecophysiological measurement system. We found that oysters successfully filtered L. *chlorophorum* cells with increased mucus secretion in all tissues analyzed. Animals previously exposed to a bloom concentration of L. *chlorophorum* exhibited significantly lower clearance rates shortly after the exposition, probably reflecting the effect of exopolymer particles produced by L. *chlorophorum* cells, and the subsequent production of mucus in the mantle and gills. However, their absorption efficiency was two-fold higher than control oysters exposed to *T. lutea*. The increase in absorption efficiency during the recovery phase could be a compensation for a decrease of clearance rate occurred during the exposure phase, interpreted as physiological depletion of *C. gigas* during green seawater discolorations. For the first time, laboratory experiments showed how high concentrations of L. *chlorophorum* can affect oyster physiology.

1. Introduction

Blooms of the marine dinoflagellate *Lepidodinium chlorophorum* (Elbrächter and Schnepf, 1996; Hansen et al., 2007) have been recorded annually along southern Brittany (North East Atlantic, France) since the last four decades and are responsible for green seawater discolorations in affected coastal areas (Sournia et al., 1992; Siano et al., 2020; Belin et al., 2021; Roux et al., 2022, 2023). Nonetheless, this phenomenon and the responsible species have been observed in estuarine-coastal waters worldwide (*e.g.*, McCarthy, 2013; Gárate-Lizárraga et al., 2014; Rodríguez-Benito et al., 2020; Siano et al., 2020; Serre-Fredj et al., 2021). Massive proliferations of L. *chlorophorum* can reach densities $>10^6$ cells L^{-1} (Sourisseau et al., 2016; Roux et al., 2022) and tend to occur particularly during the summer on the southern coast of Brittany, with maximum abundances between June–July, persisting for up to a few months (Siano et al., 2020; Belin et al., 2021; Roux et al., 2022). Although L. *chlorophorum* is not known to produce toxins (Sournia et al., 1992), green seawater discolorations could be considered harmful algae blooms (HABs), since proliferations of this dinoflagellate have been frequently associated with mass mortality events of fishes and cultured bivalves (Sournia et al., 1992; Chapelle et al., 1994; Siano et al., 2020). Recently, it was suggested that L. *chlorophorum* post-bloom hypoxic

* Corresponding author.
E-mail address: elodie.fleury@ifremer.fr (E. Fleury).

https://doi.org/10.1016/j.aquaculture.2024.740644
Received 28 September 2023; Received in revised form 22 January 2024; Accepted 2 February 2024
Available online 3 February 2024

conditions, due to the recycling of organic matter and bacterial remineralization process, might contribute to mass bivalve mortality events (Siano et al., 2020; Roux et al., 2022).

Energetic condition of marine bivalves varies with food quality and availability (Delaporte et al., 2006; Pernet et al., 2012; García-Corona et al., 2018). High abundances of some phytoplankton species can impair the feeding behavior of bivalves (Bayne, 2002), potentially by over-loading their ingestion capacity (Beninger and St-Jean, 1997) or by decreasing clearance rates (Hégaret et al., 2007). Furthermore, it has been reported that the oyster *Crassostrea gigas* could reduce its clearance, ingestion, and biodeposition rates when exposed to HABs species, such as the dinoflagellate *Alexandrium minutum* (Bougrier et al., 2003; Lassus et al., 2004; Pousse et al., 2018). In an attempt to contribute to the understanding of the main physical and chemical assumptions related to oyster's energy allocation, Pouvreau et al. (2006) developed a Dynamic Energy Budget model. This approach described the rates at which *C. gigas* could assimilate and use energy from phytoplankton to invest it in primarily physiological traits, such as growth and reproduction (Bourlès et al., 2009; Alunno-Bruscia et al., 2011; Thomas et al., 2016). The ecophysiological Dynamic Energy Budget modeling suggested that L. *chlorophorum* did not contribute to oyster's growth probably reflecting low assimilation (Pouvreau et al., 2006). However, this hypothesis still needs to be validated experimentally as *Lepidodinium chlorophorum* has an equivalent spherical diameter of 20 μm (García-Oliva et al., 2022), which corresponds to a diameter that can be filtered by *C. gigas* oysters (Dupuy et al., 2000).

Beyond its ability to form large blooms in coastal waters, another potentially harmful effect of green seawater discolorations is the excretion of large amounts of transparent exopolymer particles (TEPs) by L. *chlorophorum* cells (Claquin et al., 2008; Roux et al., 2021, 2022). TEPs are defined as particles >0.22 μm in size which may affect filtration rates in bivalves (Riisgård and Larsen, 2007). Moreover, TEPs can alter the ingestion rates of oysters, as previously observed for *C. virginica* exposed to high densities of *Aureoumbra lagunensis*, a non-toxic pelagophyceae which cause brown tides (Gobler et al., 2013; Galimany et al., 2017). Roux et al. (2022) suggested that the recycling of TEPs excreted by green seawater discolorations could accentuate hypoxia likely contributing to fauna mortalities. It is also questionable whether high TEP concentrations produced by L. *chlorophorum* could alter the filtration, ingestion, and absorption rates of the oyster *C. gigas*. To our knowledge, no study has investigated whether L. *chlorophorum* can be filtered by the oyster *C. gigas*, especially at high concentrations such as those assessed during green seawater discolorations, and whether oysters are physiologically affected by the ingestion of this dinoflagellate.

Our main objective was to investigate the ecophysiological response of the oyster *C. gigas* to L. chlorophorum exposure. We first evaluated the direct impact of the L. *chlorophorum* exposure on oyster tissues though histological analysis. Then we investigated the short-term consequences of L. *chlorophorum* exposure on oysters through measurements of clearance and respiration rates and absorption efficiency during the recovery phase. We expected that oysters exposed to L. *chlorophorum* would reduce their metabolic rate, as is usually the case with a poor quality (or toxic or fasting) diet and thus compensate during the recovery period. This experiment is the first attempt to understand to the issue oyster mortalities caused by green seawater discolorations observed in the natural environment.

2. Materials and methods

2.1. Source and management of oysters

The 195 oysters necessary for this study were produced in September 2020 at the Ifremer hatchery facilities in Argenton, France, following the procedures described by Petton et al. (2015). The juveniles (40 days old, 30.1 ± 8.4 mm, 9 ± 2.3 g) were maintained for 30 days in a 500 L nursery running system continuously supplied with filtered seawater (1 μm) at 18 ± 1 °C. The animals were daily fed with a mixed diet consisting of the Prymnesiophycidae *Tisochrysis lutea* (CCAP927/14), and the diatom *Chaetoceros gracilis* (CCAP 1010/3), 1:1 dry weight. These conditions were adapted for the animals between experiments in order to reduce the food intake according to the natural growth of the animals. More specifically, oysters were fed with the mixed diet of the two microalgae equal to 2% dry weight algae / dry weight oyster per day and per oyster (50% *Tisochrisis lutea* and 50% *Chaetoceros gracilis*), as described in Fabioux et al. (2005).

2.2. Microalgae cultures

The dinoflagellate L. *chlorophorum* strain RCC6911 (RCC: Roscoff Culture Collection; http://roscof-culture-collection.org/) isolated in the Vilaine Bay (southern Brittany, France) in 2019 was grown in several 500 mL batch cultures using autoclaved filtered (1 μm) seawater supplemented with L1 medium (Guillard and Hargraves, 1993) for a total of 120 L of culture (40 L per experiment) which was the maximum feasible volume for the laboratory facilities. Cultures were maintained at 21 ± 1 °C and 70 μmol photon m^{-2} s^{-1}, with a dark: light cycle of 12:12 h.

The strains of *T. lutea* were obtained from the Argenton hatchery (Ifremer – France) and cultures were produced in 300 L cylinders containing 1 μm-filtered seawater enriched with Conway medium (Walne, 1970) and maintained at 22 ± 1 °C, air-CO_2 (0.45%), and continuous aeration and light (78 μmol photon m^{-2} s^{-1}). Both cultures (*L. chlorophorum* and *T. lutea*) were harvested in the exponential growth phase (8 days; ~ 13 × 10^3 cells mL^{-1}, and 6 days; ~ 9000 × 10^3 cells mL^{-1}, respectively) for the feeding experiments.

2.3. Experimental design

2.3.1. Exposure experiment

On the 12th April 2021, a laboratory experiment was performed 1) to determine whether the oysters could filter cells of L. *chlorophorum* and, 2) to investigate the impact of the dinoflagellate on oyster's physiology (Fig. 1). Our experimental design consists of two phases: an initial exposure of 48 h to different diets followed by a recovery period of 24 h under a standard diet. Prior to the start of experiment, initial biometric analyses (length, width, fresh and dry flesh, and shell weight) were performed ($N = 10$; Table S1). Oysters were fasted for 72 h to clear their gut and randomly placed in tanks and exposed to different diets.

For the exposure phase, 65 oysters were placed in 7 L tanks and exposed to three feeding conditions (Fig. 1A): 1) a control condition with *T. lutea* (59,796 cells mL^{-1}; *T. lutea*), 2) *L. chlorophorum* in low concentration (640 cells mL^{-1}; *L. chlorophorum*-low), corresponding to the same bio-volume as *T. lutea* and, 3) *L. chlorophorum* in high concentration (7440 cells mL^{-1}; *L. chlorophorum*-bloom). For each feeding condition, an additional tank, without oysters, was used as control in order to follow the growth dynamic of phytoplankton cultures throughout the experiment (Fig. 1A). All tanks were equipped with a pump (Aquapower 200, SuperFish, at 200 L h^{-1}) to limit the sedimentation of phytoplankton cells, and an oxygen bubbler (Hobby; 50 mm). The temperature of the room was 20 ± 1 °C and light was continuous (78 μmol photon m^{-2} s^{-1} on average in the room). The oysters were fed twice daily, 5 h apart. Seawater temperature, salinity, pH, oxygen saturation and phytoplankton cell concentrations were measured every 10 min for 90 min after each feeding (0 h, 5 h, 24 h and 29 h) both in the oyster tanks and in the control tanks (Fig. 1). In order to estimate the photo-physiological status of phytoplankton cells, the maximum quantum efficiency of the photosystem II was measured at the beginning and end of each feeding as well as TEP concentrations (Fig. 1B). In addition, ten oysters per condition were randomly collected for histological analysis after 48 h of exposure (N = 10; Fig. 1B).

For the recovery phase, oysters previously exposed to the different diets were placed in individual chambers of an ecophysiological measurement system (Pousse et al., 2018). This system allows to measure

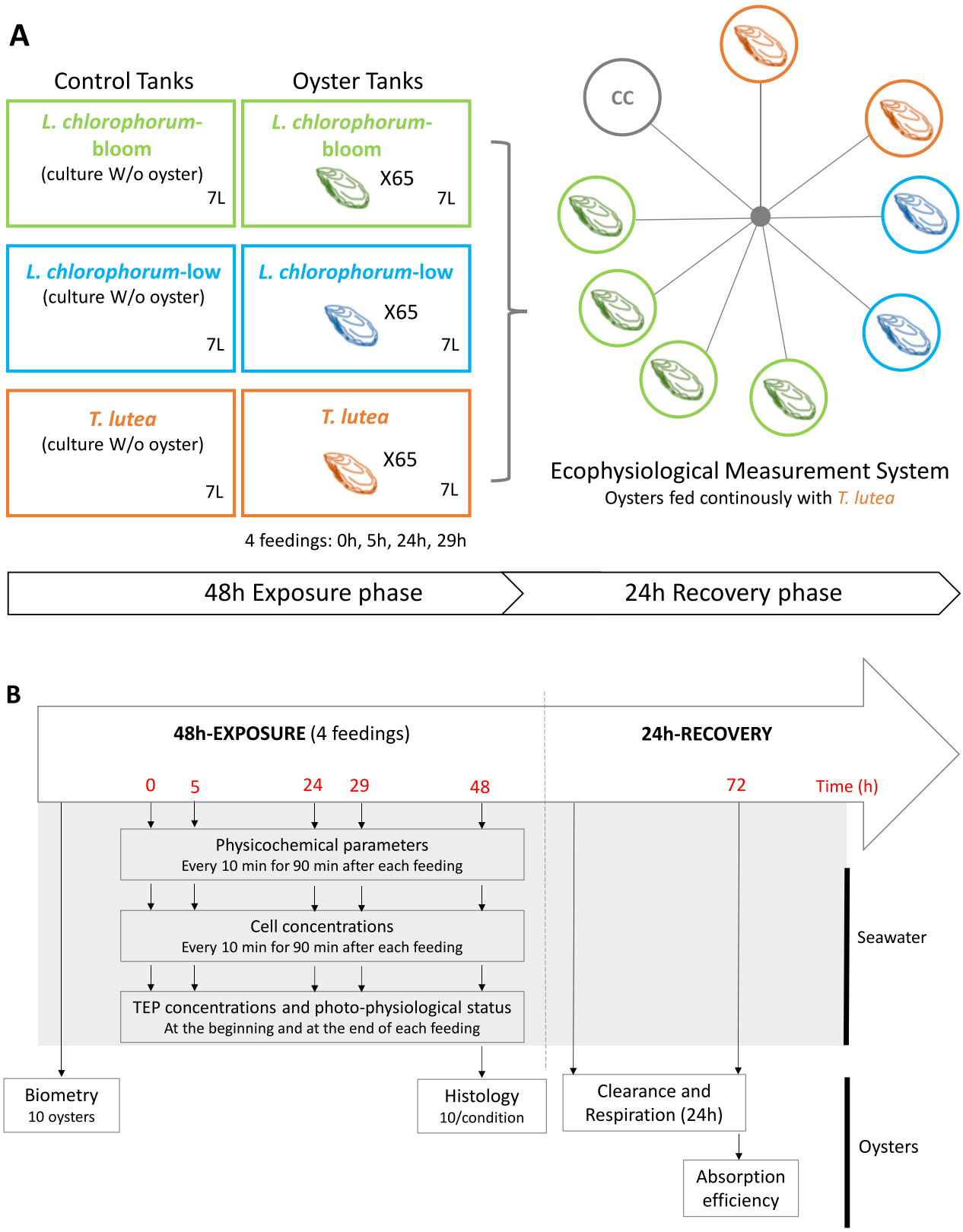

Fig. 1. Experimental design (A) and sampling schedule (B). Feedings were represented as follows: 0 h, 5 h, 24 h and 29 h. The 48 h-exposure phase consists of three tanks containing oysters corresponding to three food regimes (*L. chlorophorum*-bloom, *L. chlorophorum*-low and *T. lutea*), and three control tanks without oysters. The direct impact of L. *chlorophorum* on oysters was assessed through histological analysis (48 h). During the 24 h-recovery phase, oysters were fed continuously with *T. lutea* within an ecophysiological measurement system composed of nine individual chambers (including one control chamber without oyster (CC)). Clearance and respiration rates as well as absorption efficiency were measured individually to assess the short-term consequences of a L. *chlorophorum* exposure on oyster ecophysiology.

continuously physiological rates of eight individual oysters and one control blank (without oyster). The tested oysters were continuously fed with *T. lutea* to measure the consequence of prior exposures on individual clearance and respiration rates, and absorption efficiency. Oysters previously exposed to *T. lutea* ($N = 2$), *L. chlorophorum*-low (N = 2), *L. chlorophorum*-bloom ($N = 4$) were studied (Fig. 1).

2.3.2. Additional experiments

Additional experiments were conducted under similar environmental conditions to increase the number of replicates available for recovery analysis (Fig. S1). Before the start of each additional experiment, we verified that oysters had similar morphological characteristics (ANOVA, $P > 0.05$, $N = 5$–10; Table S1).

On the 16th March 2021 (Fig. S1A), 65 oysters were placed in 7 L tanks and exposed to *T. lutea* (59,276 cells mL^{-1}) or L. *chlorophorum*-low (622 cells mL^{-1}) conditions. For the recovery phase, oysters previously exposed to *T. lutea* ($N = 3$) and L. *chlorophorum*-low (N = 3) were investigated (Fig. S1A).

Finally, an additional experiment was conducted on the 27th April 2021 (Fig. S1B). Due to the limited amount of L. *chlorophorum* available, only 25 oysters were placed in 3.5 L tanks and exposed to the three feeding conditions: *T. lutea* (52,058 cells mL^{-1}), *L. chlorophorum*-low (742 cells mL^{-1}), *L. chlorophorum*-bloom (7148 cells mL^{-1}). For the recovery phase, oysters previously exposed to *T. lutea* ($N = 8$), *L. chlorophorum*-low (N = 8) and *L. chlorophorum*-bloom (N = 8) were studied (Fig. S1B).

2.4. Environmental parameters

Temperature (°C), pH, salinity (PSU), and oxygen saturation (%) were measured using a multi-parameter probe (WTW Multi 3430) in all tanks during the 48 h of exposure to ensure that environmental conditions were favorable for the development of oysters. After each feeding, we estimate phytoplankton cell concentrations in each tank ($\mu m^3\ mL^{-1}$) using a Beckman Coulter Multisizer (range: 0–200 μm^3 for *T. lutea,* and 400–6000 μm^3 for L. *chlorophorum*). Furthermore, the photo-physiological status of phytoplankton cells was controlled by measuring the maximum quantum efficiency of the photosystem II at 455 nm (Flash Pulse = 20%), using an Aquapen-C 100 fluorimeter (Photon Systems Instruments), maintaining 3 mL by triplicate in the dark for 15 min (Kromkamp and Forster, 2003), before measurement.

The concentration of TEPs was determined using a semi-quantitative method based on the colorimetric determination of the amount of dye conjugated with extracellular particles (Claquin et al., 2008 adapted from Passow and Alldredge, 1995). Briefly, triplicate samples of 20 mL of seawater were gently filtered through 0.4 μm polycarbonate membrane filters (Whatman® Nuclepore™ Track-Etched Membrane). Subsequently, particles retained on the filter were stained with Alcian Blue solution (Sigma). After one night of drying at 50 °C, 6 mL of 80% H_2SO_4 were added, and 2 h later, the absorption of the supernatant was measured using a spectrometer at 787 nm (Shimadzu UV-2600). Alcian blue absorption was calibrated using a solution of Xanthan gum. The TEP concentrations were expressed in $\mu g\ Xeq\ L^{-1}$.

2.5. Semiquantitative histochemistry

After 48 h of exposure 10 oysters per feeding condition were sampled ($N = 10$). The meat was carefully excised from the shell, and cross-sections of the mid-visceral mass (~1 mm^3) from each oyster were fixed in Davidson solution (Kim et al., 2006) for 48 h, and preserved in ethanol 70% until processing. Tissue samples were dehydrated in ethanol, embedded in paraffin (Paraplast Plus, Leica Biosystems, Richmond, IL, USA), and thin-sectioned (4-μm) using a rotary microtome (Leica RM 2155, Wetzlar, DE). Then, sections were mounted on glass slides, deparaffinized and cleared in xylene, and rehydrated in regressive series of ethanol before staining.

A series of 2 consecutive sections were performed for each sample, which were used for (i) multichromic staining using a combination of Alcian Blue and Periodic Acid-Schiff's for the demonstration of acid mucopolysaccharides and neutral glycoconjugates, in blue and magenta tones, respectively, and hematoxylin blueing for nuclear materials (Costa and Costa, 2012; García-Corona et al., 2022), and (ii) Hematoxyline/eosin staining (Kim et al., 2006) to analyze the general morphology and potential histopathologies of the tissues. Slides were mounted in DPX resin and examined under a Zeiss Axio Observer Z1 light microscope.

The histological sections stained with the multichromic technique were digitalized at high resolution (600 dpi; 40×), and three randomly selected images from each tissue (mantle, gills, stomach, intestine, and digestive gland) were processed with the Image-Pro Premier v.9.0 software (Media Cybernetics, Bethesda, MD, USA). The software relies on automatic calculations of the area occupied by acid and neutral glycoconjugates (Díaz et al., 2008) based on the segmentation of pixels in the image in relation to the intensity of the specific colour of each biochemical component according to the staining procedure mentioned above (Rodríguez-Jaramillo et al., 2008). The Acid GLycoConjugates index (AGLC) and the Neutral GLycoConjugates index (NGLC) were calculated based on the formula described by García-Corona et al. (2018):

$$\mathrm{AGLC/NGLC}\,(\%) = \frac{\text{area occupied by acid or neutral glycoconjugates}}{\text{area occupied by the tissues}} \times 100.$$

Furthermore, a three-level semi-quantitative scale (0 = absent, 1 = low presence, 2 = moderate presence, and 3 = high presence) was established to assess the intensity of the histopathological features evaluated on the different tissues of the oysters, as described in Fabioux et al. (2005).

2.6. Ecophysiological measurements

We overall measured the individual clearance ($L\ h^{-1}\ g^{-1}$ dw std) and respiration ($mg\ O_2\ h^{-1}\ g^{-1}$ dw std) rates of oysters after 48 h of exposition to *T. lutea* ($N = 13$), *L. chlorophorum*-low (N = 13) and L. *chlorophorum*-bloom ($N = 12$). The ecophysiological measurement system consists of nine identical 0.54 L flow-through acrylic chambers supplied with *T. lutea* culture pumped from a tank (Pousse et al., 2018). Each chamber contained one single oyster, except for an empty chamber kept as a control (Fig. 1A). Flow rate in the chamber was adjusted to 40 mL min^{-1} using two peristaltic pumps (Masterflex L/S 7551, Cole Parmer, USA). The temperature (°C) and fluorescence (FFU) of the seawater were measured for 15 min in the outflow of each chamber using a WTW multiparameter meter (WTW Multi 3430) and a fluorometer (WETstar chlorophyll, WETLABS, Philomath, USA), respectively. Calibration lines obtained from cell counts allowed recalculating phytoplankton cell concentrations from fluorescence values. These instruments were connected to a computer for the visualization and acquisition of high-frequency time series data. The fluorescence of the water out-flowing from chambers was monitored sequentially for a 15 min cycle. This protocol allowed the monitoring of each chamber every 3.5 h for 24 h.

For each chamber, the individual clearance rate (*CR*) of each oyster was estimated as:

$$CR = fl \times \frac{(C_{CC} \times C_N)}{C_{CC}}$$

where *fl* is the flow rate through the chamber (Lh^{-1}), C_{CC} is the concentration of phytoplankton in the control chamber (*CC*) and C_N is the concentration of phytoplankton in a chamber with an oyster (Bayne, 2017; Tallec et al., 2021).

The individual respiration rate (*RR*) is defined as:

$$RR = fl \times (O_{CC} \times O_N)$$

where *fl* is the flow rate through the chamber (L h^{-1}), O_{CC} and O_N are the concentrations of O_2 (mg O^2 L^{-1}) in the control chamber and in a chamber with the oyster, respectively (Savina and Pouvreau, 2004; Tallec et al., 2021). At the end of each run, oysters were sacrificed and stored at −20 °C before measuring the dry flesh weight in order to calculate mass standardized clearance and respiration rates for an equivalent individual of 1 g dry tissue (Bayne et al., 1987; Tallec et al., 2021).

After 24 h, absorption efficiency (*AE*, %) of organic matter (OM) from ingested *T. lutea* cells ($OM_{T.lutea}$ = 94%) was calculated according to Conover's method by collecting feces from each chamber:

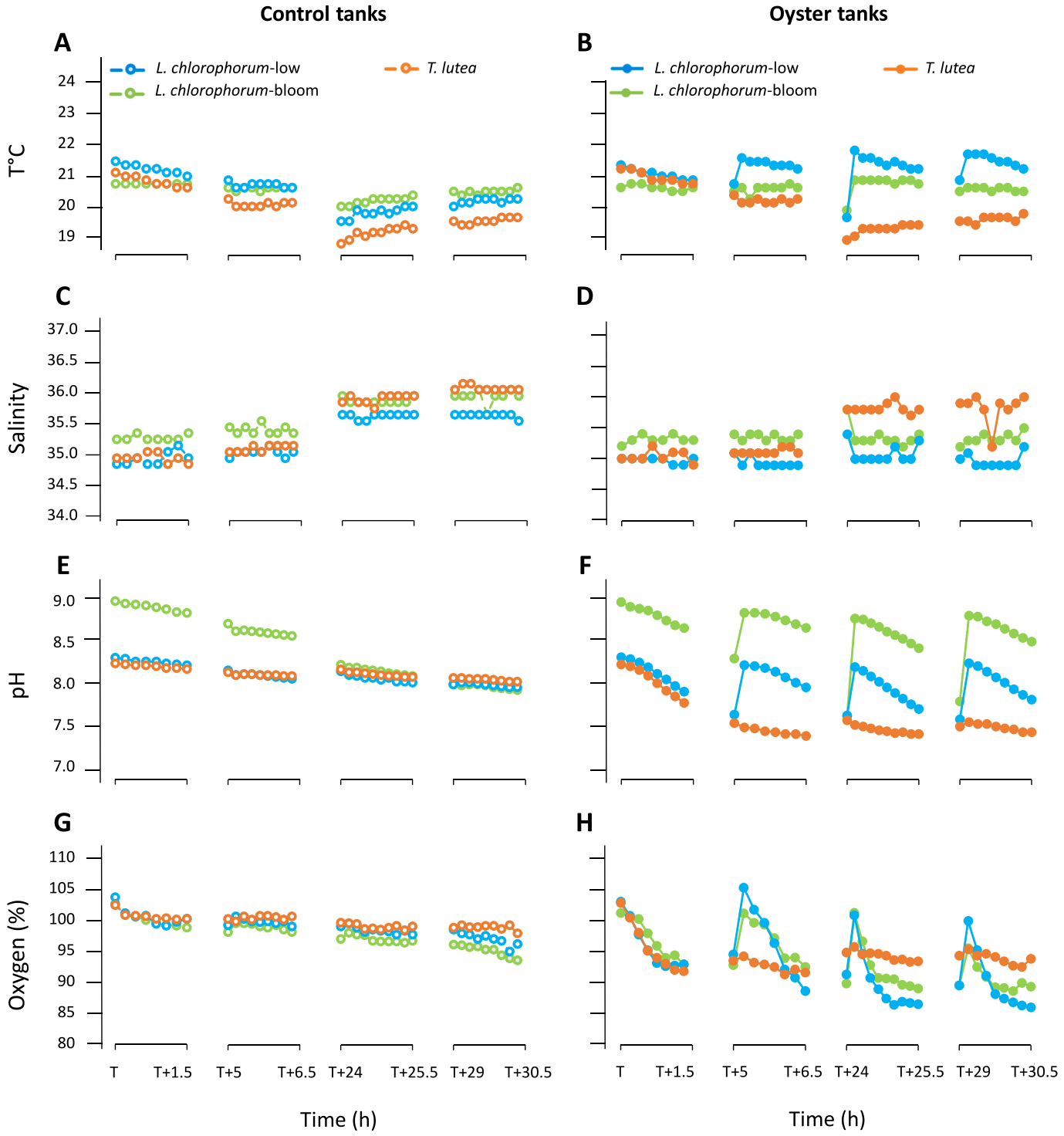

Fig. 2. Variations in physicochemical parameters recorded during the exposure experiment: temperature (°C; A, B), salinity (C, D), pH (E, F) and oxygen saturation (%; G, H) in the control tanks (without oysters; open symbols) and in the oyster tanks (containing oysters; filled symbols). After each feeding (*T* = 0 h, T + 5 h, T + 24 h, T + 29 h), parameters were recorded every 10 min for 90 min. Feeding conditions are represented as follows: *L. chlorophorum* bloom concentration (*L. chlorophorum*-bloom; green circles), *L. chlorophorum* in low concentration (*L. chlorophorum*-low; bleu circles) and *T. lutea* (orange circles). (For interpretation of the references to colour in this figure legend, the reader is referred to the web version of this article.)

$$AE = \frac{f - e}{(1 - e) \times f} \times 100$$

where f corresponds to the organic fraction of the diet and e is the organic fraction of the feces (Conover, 1966; Iglesias et al., 1998).

2.7. Statistical analysis

The data were statistically analyzed using command lines in the R language (R v. 4.0.2, R Core Team, 2020). Shapiro–Wilk and Bartlett tests were applied to confirm the normality of frequencies and homogeneity of variances of the residuals of the data, respectively (Hector, 2015). Separate unifactorial analyses of variance (ANOVA) and Chi-square test (χ^2) were applied to each tissue of analyzed by histochemistry to detect significant differences in quantitative indices (AGLC and NGLC), and histopathological features, respectively, as a function of the three experimental food regimes. As needed, Tukey's HSD test were applied to identify differences between means (Zar, 2010). Mixed model ANOVAs were performed to determine differences in the clearance and respiration rates as a function of food regime, time and experiment. Main factors were food regime (*L. chlorophorum*-low, *T. lutea*, *L. chlorophorum*-bloom) and time. The experiment was considered as a random factor. The repeated option was applied to the time to take into account temporal dependence. Furthermore, a one-way ANOVA was run to measure significant differences in the food-absorption efficiency data as a function of food regime. Prior to analysis, an angular transformation (arcsine $\sqrt{P}$) was applied to the values expressed in percentages, but data are reported untransformed as the mean ± standard deviation (SD) except when indicated. The level of statistical significance was set at $P < 0.05$ for all analyses (Zar, 2010).

3. Results

3.1. Physicochemical parameters

Physicochemical parameters were monitored in the six tanks (three oyster tanks and three control tanks without oysters) for each food-regime during the 48 h of the exposure experiment (Fig. 2). Temperature and salinity remained stable during the 48 h in both controls and treatments, with values of 20.6 ± 0.6 °C (Fig. 2A, B) and 35.4 ± 0.4 (Fig. 2C, D), respectively. As shown in Fig. 2E, no major changes were observed in the pH of the control tanks during the 90 min after each feeding, nonetheless, values of pH decreased according to respiration and consumption of phytoplankton cells by the oysters (Fig. 2F). Oxygen saturation remained stable for the three control tanks (98.7 ± 1.8%, Fig. 2G). In contrast, oxygen showed a higher temporal variability in the L. *chlorophorum*-low and L. *chlorophorum*-bloom conditions, ranging from 86.1% to 105.3% (Fig. 2H).

3.2. Phytoplankton and TEP concentrations

Microalgae concentrations in the controls were up to 10-fold higher in the L. *chlorophorum*-bloom condition than in the L. *chlorophorum*-low and *T. lutea* conditions during the first 24 h of the exposure experiment

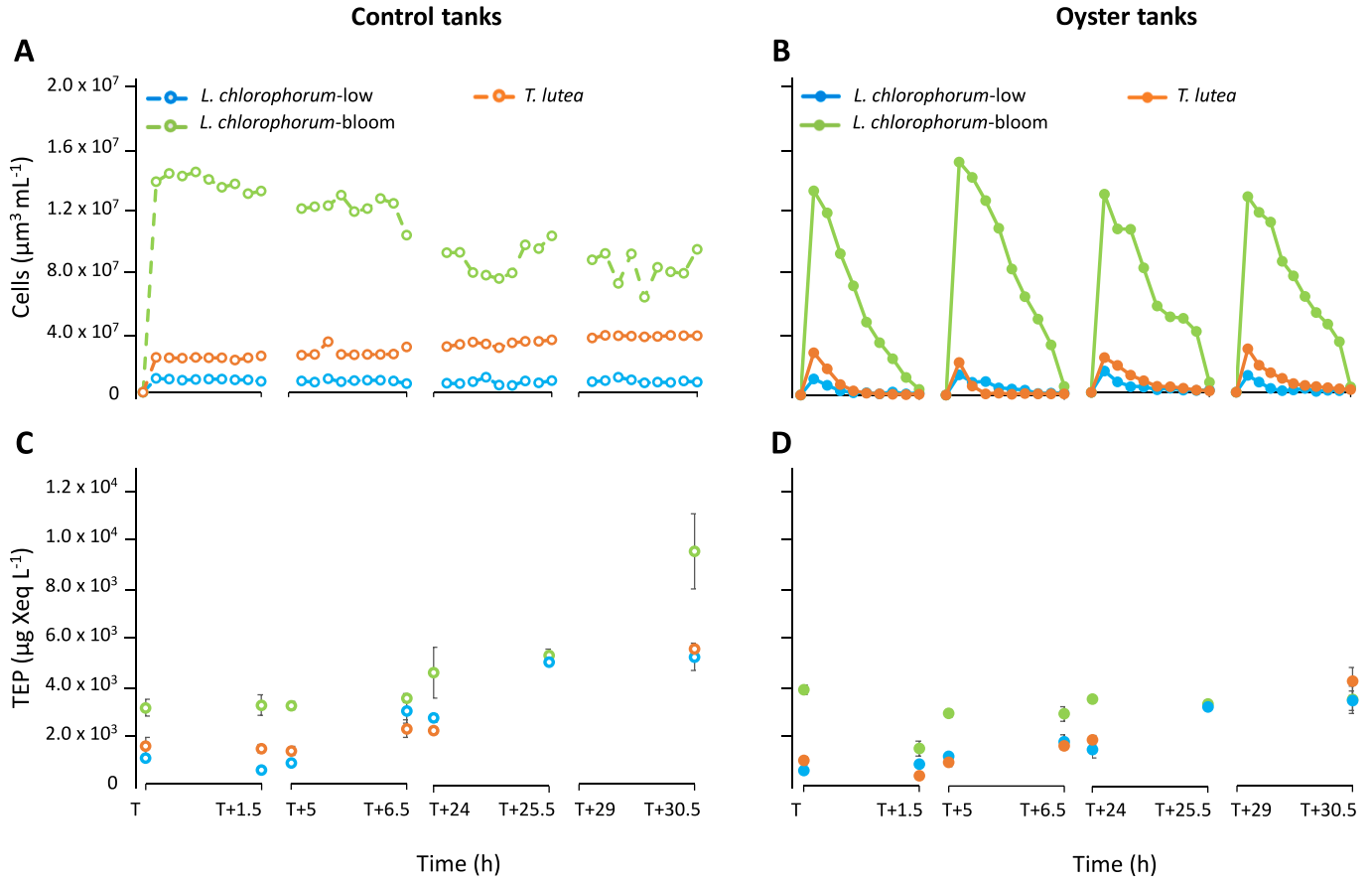

Fig. 3. Total phytoplankton (µm^3 mL^{-1}; A, B) et TEP concentrations (µg Xeq L^{-1}; C, D) measured during the exposure experiment in the control tanks (without oysters; open symbols) and in the oyster tanks (containing oysters; filled symbols). Cell concentration was recorded every 10 min for 90 min following each feeding (T = 0 h, T + 5 h, T + 24 h, T + 29 h) and TEP concentration was measured only at the beginning and end of each feeding. Feeding conditions are represented as follows: *L. chlorophorum* bloom concentration (*L. chlorophorum*-bloom; green circles), *L. chlorophorum* in low concentration (*L. chlorophorum*-low; bleu circles) and *T. lutea* (orange circles). (For interpretation of the references to colour in this figure legend, the reader is referred to the web version of this article.)

(Fig. 3A). Nonetheless, after 90 min of each feeding, cell concentration drastically decreased in the oyster tanks from $14 \times 10^6 \pm 1.6 \times 10^6$ µm^3 mL^{-1} to $0.49 \times 10^6 \pm 0.16 \times 10^6$ µm^3 mL^{-1} in the *L. chlorophorum*-bloom condition (Fig. 3B). Similarly, cell concentration decreased from $1.3 \times 10^6 \pm 0.18 \times 10^6$ µm^3 mL^{-1} to $0.17 \times 10^6 \pm 0.071 \times 10^6$ µm^3 mL^{-1} in the *L. chlorophorum*-low condition, and from $2.6 \times 10^6 \pm 0.36 \times 10^6$ µm^3 mL^{-1} to $0.11 \times 10^6 \pm 0.048 \times 10^6$ µm^3 mL^{-1} in the *T. lutea* condition (Fig. 3B). For the three conditions, oysters filtered >85% of the available phytoplankton prior the subsequent feeding (Fig. 3B). On the other hand, the maximum quantum efficiency of the photosystem II was 0.6 ± 0.1 for L. *chlorophorum* cultures, and 0.7 ± 0.0 for *T. lutea* throughout the experiment (data not shown), which indicates the good physiological state of the algae during experimental conditions.

In the control tanks, TEP concentration increased steadily over time (Fig. 3C), with the maximum values measured in the L. *chlorophorum*-bloom condition after 48 h (9,681 ± 1566 µg Xeq L^{-1}). These values were twice higher as those recorded in the L. *chlorophorum*-low and *T. lutea* conditions at the end of the exposure experiment (Fig. 3C). In the oyster tanks (Fig. 3D), a constant increase in TEP concentrations was observed up to highest levels in the L. *chlorophorum*-low (621 ± 35 to 3527 ± 402 µg Xeq L^{-1}) and *T. lutea* conditions (1034 ± 161 to 4331 ± 577 µg Xeq L^{-1}) after 48 h of exposure. Notwithstanding, during the first 24 h of exposure, TEP concentrations were higher in the L. *chlorophorum*-bloom condition (3031 ± 936 µg Xeq L^{-1}) than in the *L. chlorophorum*-low and *T. lutea* conditions (1217 ± 483 µg Xeq L^{-1}, and 1201 ± 605 µg Xeq L^{-1}, respectively). Afterwards, TEP's in the *L. chlorophorum*-bloom condition decreased by 60% after 90 min of the first feeding, and remained stable until the end of the exposure experiment (3327 ± 245 µg Xeq L^{-1}, Fig. 3D).

3.3. Histochemical analysis after exposure

The microanatomical inspection of the oysters collected after 48 h of exposure to the three different food-regimens allowed to observe the presence of some histopathologies, as well as the production of acid glycoconjugates (AGLC = mucus) and the storage of neutral glycoconjugates (NGLC = glycogen) in some tissues such as the mantle, gills, stomach, intestine, and digestive gland (Fig. 4A-O). In the mantle, the strongest amount of mucus-producing globose cells was observed in oysters exposed to the L. *chlorophorum*-bloom condition (Fig. 4A), while the presence of glycogen granules was observed in the vesicular connective tissue of animals fed with *T. lutea* (Fig. 4C). A similar pattern was found in the gills, with the highest number of mucus cells in the gill filaments of oysters exposed to the *L. chlorophorum* bloom (Fig. 4D) and the lowest in animals exposed to *T. lutea* (Fig. 4F).

As shown in Fig. 4G and I, a significant hemocytic infiltration was found in the stomach epithelium of oysters fed with the L. *chlorophorum*-bloom and *T. lutea* regimens, with an important mucus production by the globose cells in oysters exposed to L. *chlorophorum* bloom (Fig. 4G). In the intestinal epithelium, a large amount of mucus-producing cells was observed in the conditions where the oysters were exposed to L. *chlorophorum* cells (Fig. 4J-K), while the inclusion of glycogen granules in the intestinal epithelium was found in the oysters fed with the *L. chlorophorum*-bloom diet (Fig. 4J). Finally, as seen in Figs. 4M-N, the strongest amounts of AGLC was found in the digestive cells of the digestive diverticula of oysters exposed to L. *chlorophorum*. Notwithstanding, no globose mucus-producing cells were observed embedded in the epithelium of the digestive diverticula. Whereas the presence of NGLC was mainly observed in the digestive glands of oysters fed with the *L. chlorophorum*-bloom and *T. lutea* regimens (Fig. 4M and O, respectively).

After a semiquantitative immunohistochemical evaluation, no differences ($P > 0.05$) were found in the deformation and vacuolation in the epithelia of any of the tissues between the different experimental conditions analyzed in this work (Table 1). Nonetheless, a significant hemocyte infiltration was measured in the stomach epithelium of oysters exposed to the *L. chlorophorum*-bloom and *T. lutea* feeding regimes (Table 1). The highest amounts ($P < 0.05$) of AGLC were found in the mantle, gills, stomach, and digestive gland of oysters fed with the *L. chlorophorum*-bloom diet, where the digestive gland was the organ with the highest AGLC index, followed by the intestine and stomach (Table 1). Furthermore, as shown in Table 1, the highest amounts of NGLC were observed in the stomach, intestine, and digestive gland of oysters fed with the *L. chlorophorum*-bloom diet, while the largest amounts ($P < 0.05$) of NGLC in the mantle where quantified in animals fed with *T. lutea*.

3.4. Ecophysiological response during recovery

Food and time interacted in their effect on clearance rate (Table S2). At the beginning of the recovery phase, clearance rate was 2.3–2.7 time higher in the *T. lutea* condition than in the L. *chlorophorum*-low and L. *chlorophorum*-bloom conditions (Fig. 5A). Clearance rate of oysters in the *T. lutea* condition declined gradually throughout the experiment and became similar to that observed in the other conditions after 11 h for which it was stable (Fig. 5A). The respiration rate varied as a function of time and food regime (Table S2 and Fig. 5B). Respiration was stable throughout the recovery period but increased slightly at the end (Fig. 5B). Overall, respiration rate of oysters was lower in animals fed L. *chlorophorum*-low. Finally, absorption efficiency of oysters previously exposed to L. *chlorophorum*-bloom and L. *chlorophorum*-low conditions was twice as high as that of the *T. lutea* condition ($P < 0.05$; Fig. 6).

4. Discussion

For the first time, we suggest that the oyster successfully filters and ingests L. *chlorophorum* but there is a physiological cost to this. In particular, we have observed that this dinoflagellate produces TEPs which may be the cause of a decrease in filtration activity and generalized tissue lesions, with a negative impact on energy reserves.

Here we show that L. *chlorophorum* produces TEPs but still, oysters can ingest the dinoflagellate. However, it has been documented that benthic suspension feeders are capable to produce significant amounts of TEPs under field and laboratory conditions (Li et al., 2008), such as the oyster *C. virginica* (McKee et al., 2005). While TEP production by *C. gigas* cannot be completely excluded, the concentrations measured in the control tanks allowed to confirm that L. *chlorophorum* was the main producer of TEPs during the experiment, without the inhibition of filtration rates in L. *chlorophorum*-bloom condition after 48 h. Nevertheless, these results were obtained under controlled conditions, with sequential feedings. In estuarine-coastal ecosystems, biological and physical processes can deeply affect the coagulation of TEPs (Alldredge et al., 1993; Passow et al., 2001) and therefore strongly modify the particles size spectrum available for oysters during a green seawater discoloration. Hence, the ecophysiological response observed in this work remains to be confirmed under green seawater discolorations in the field.

There is evidence that HABs may cause histopathological lesions in exposed bivalves (Estrada et al., 2010; Hégaret et al., 2012; Lassudrie et al., 2020; García-Corona et al., 2022). The most common histopathological alterations observed in bivalve tissues are sudden increases in hemocyte infiltration, cellular apoptosis, autophagy, and vacuolation (Estrada et al., 2010; Hégaret et al., 2010, 2012; García-Corona et al., 2022; Rodríguez-Jaramillo et al., 2022), as well as melanization of gills and mantle, edema, delamination and atrophy of the digestive tubules (Estrada et al., 2010; Haberkorn et al., 2010; Medhioub et al., 2012; Lassudrie et al., 2014; Neves et al., 2019), and mucus production through epithelial irritation (Gao et al., 2021). In the present study, the exposition to the non-toxic dinoflagellate L. *chlorophorum* induced some histopathological lesions (mainly hemocyte infiltration, as well as deformation and vacuolation of epithelia) in different tissues of the oysters; but no significant differences were observed in the intensity of

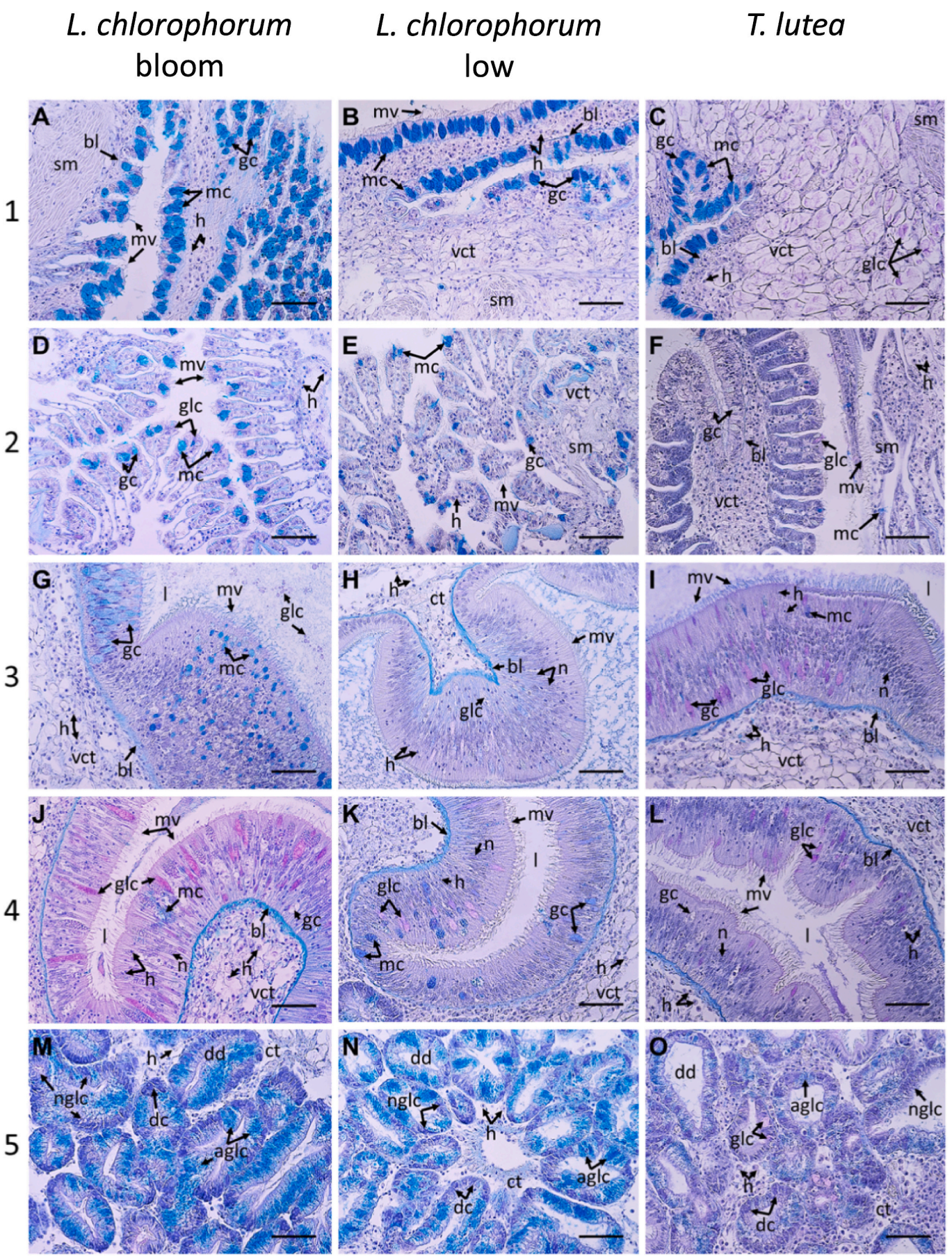

(caption on next page)

Fig. 4. Microphotograps of the tissues (1 = mantle, 2 = Gills, 3 = stomach, 4 = intestine, 5 = digestive gland) of oysters *C. gigas* after 48 h of *in vivo* exposure to artificial blooms of the green dinoflagellate *L. chlorophorum* (*L. chlorophorum*-bloom; *N* = 10), *L. chlorophorum* in low concentration (*L. chlorophorum*-low; N = 10) and *T. lutea* (N = 10). bl, basal lamina; ct, connective tissue; dc, digestive cells; dd, digestive diverticula; gc, globose cells; glc, acid glycoconjugates; glc, glycogen; h, hemocytes; l, lumen; mc, mucus cells; mv, microvilli; n, nucleus; ngcl, neutral glycoconjugates; sm, smooth muscle; vct, vesicular connective tissue. Multichromic histochemical staining for the demonstration of glycogen (magenta patches), neutral glycoconjugates (violet tones), acid glycoconjugates (blue hues), and proteins (yellowish dyes). Scale bar: 40 × = 50 μm. (For interpretation of the references to colour in this figure legend, the reader is referred to the web version of this article.)

these lesions among food regimes.

Notwithstanding, the histochemical analysis revealed an inflammation and mechanical stress through the significant mucus production in most of the tissues of oysters exposed to L. *chlorophorum* in both L. *chlorophorum*-bloom and *L. chlorophorum*-low conditions, particularly in those tissues that represent a primary barrier to the environment (mantle and gills), where the highest proliferation of mucus-producing cells was observed. The production of mucus by marine invertebrates has been commonly interpreted as an innate response to stressful environmental conditions, like exposure to pathogens or contaminants (Izzetoğlu et al., 2014; Martins et al., 2014; Ghosh, 2020), but this histopathology has been also documented as a sign of mechanical stress in *C. gigas* after the exposure to HABs of the toxic dinoflagellate *Alexandrium catenella* (Gao et al., 2021). Additionally, high amounts of acid glycoconjugates were observed in the cytoplasm of the digestive cells of oysters exposed to *L. chlorophorum* in this work. Since the presence of mucus-producing globose cells embedded in the epithelium of the digestive diverticula was not observed, the blue staining in the digestive glands of *C. gigas* could be attributed to the ingestion of the significant amounts of TEPs produced by L. *chlorophorum*. Indeed, Gobler et al. (2008) found that the presence of the brown dinoflagellate *Cochlodinium polykrikoides* induced an inflammatory response in tissues of several shellfish species, which might be related to the extracellular polysaccharides produced by harmful phytoplankton. This evidence suggests that the ingestion of TEPs produced during green seawater discolorations could trigger an inflammatory response in the digestive glands of affected *C. gigas*. Further research is needed to strengthen this idea.

To our knowledge, this is the first evidence suggesting that massive proliferations of L. *chlorophorum* can be detrimental to the physiological state of *C. gigas*. It is also important to highlight that oysters were exposed to relatively low cell densities compared to those generally used under experimental approaches to assess the negative impacts of dinoflagellates on oyster tissues (Hégaret et al., 2010, 2012); nonetheless, the concentrations of L. *chlorophorum* used in this study were similar to those recorded *in situ* during green seawater discolorations. Furthermore, it cannot be completely excluded that a longer exposure to L. *chlorophorum* (up to several weeks as occurs during green seawater discolorations) could potentially induce microanatomical lesions on *C. gigas* tissues.

The histochemical analyses revealed significantly higher amounts of neutral glycoconjugates (= glycogen) in the digestive tissues of oysters exposed to the L. *chlorophorum*-bloom condition. In marine bivalves, the assimilation and transport of food-nutrients is mediated by the hemocytes mainly in the digestive epithelia during periods of high food availability (Gabbott, 1975; Barber and Blake, 2006). These results confirms that the oysters were able to ingest L. *chlorophorum* cells in the same way as the cells of *T. lutea*. Nevertheless, in some species with a conservative strategy (López-Carvallo et al., 2017; García-Corona et al., 2018), and particularly in *C. gigas* (Rodríguez-Jaramillo et al., 2008, 2022), the storage of energy substrates, such as glycogen, occurs primarily in the mantle to fuel growth and reproduction. Thus, finding significantly lower amounts of glycogen granules in the mantle of oysters from the L. *chlorophorum*-bloom condition than in those fed with *T. lutea* suggest that the phytoplankton-ingestion in animals exposed to L. *chlorophorum* did not contribute equally to energy reserves. These findings represent an innovative result compared to the current literature, and corroborate the previous hypothesis based on the Dynamic Energy Budget model, suggesting that oysters have a low food-nutrient absorption efficiency from L. *chlorophorum* (Pouvreau et al., 2006; Bourlès et al., 2009; Alunno-Bruscia et al., 2011; Thomas et al., 2016). To validate this hypothesis, further analysis of the nutritional value of L. *chlorophorum* cells and bioenergetics of *C. gigas* during green seawater discolorations are needed.

Several studies have investigated the direct impact of HABs exposure

Table 1
Mean histopathological and histochemical (AGLC = acid glycoconjugates index, NGLC = neutral glycoconjugates index) changes in the tissues of oysters *C. gigas* (*n* = 30) after 48 h of *in vivo* exposure to artificial blooms of the green dinoflagellate L. *chlorophorum* (*L. chlorophorum*-bloom), *L. chlorophorum* in low concentration (*L. chlorophorum*-low) and *T. lutea*.

Tissue	Feature	Condition			Statistical analysis	
		L. chlorophorum-bloom	*L. chlorophorum*-low	*T. lutea*		
Mantle	Deformation	0.5 ± 0.2^{a}	1.1 ± 0.2^{a}	0.8 ± 0.3^{a}	$\chi^2_{(df=6)} = 4.5$	$P = 0.338$
	Vacuolation of the epithelium	1.2 ± 0.3^{a}	2.0 ± 0.3^{a}	1.4 ± 0.3^{a}	$\chi^2_{(df=6)} = 6.0$	$P = 0.423$
	AGLC (%)	$\mathbf{14.5 \pm 1.7^{a}}$	$\mathbf{9.1 \pm 1.2^{b}}$	$\mathbf{5.7 \pm 1.3^{b}}$	$\mathbf{F_{(df=2)} = 37.8}$	$\boldsymbol{P = 0.000}$
	NGLC (%)	$\mathbf{2.9 \pm 0.4^{b}}$	$\mathbf{2.6 \pm 0.3^{b}}$	$\mathbf{12.7 \pm 1.2^{a}}$	$\mathbf{F_{(df=2)} = 26.6}$	$\boldsymbol{P = 0.000}$
Gills	Vacuolation	0.6 ± 0.2^{a}	0.7 ± 0.3^{a}	1.0 ± 0.3^{a}	$\chi^2_{(df=6)} = 2.7$	$P = 0.841$
	Hemocyte infiltration	1.2 ± 0.2^{a}	1.0 ± 0.4^{a}	0.9 ± 0.2^{a}	$\chi^2_{(df=6)} = 8.9$	$P = 0.175$
	AGLC (%)	$\mathbf{19.8 \pm 2.5^{a}}$	$\mathbf{4.2 \pm 0.5^{b}}$	$\mathbf{3.5 \pm 0.5^{b}}$	$\mathbf{F_{(df=2)} = 37.5}$	$\boldsymbol{P = 0.000}$
	NGLC (%)	$\mathbf{0.3 \pm 0.2^{b}}$	$\mathbf{0.0 \pm 0.0^{b}}$	$\mathbf{3 \pm 0.5^{a}}$	$\mathbf{F_{(df=2)} = 26.7}$	$\boldsymbol{P = 0.000}$
Stomach	**Hemocyte infiltration**	$\mathbf{1.9 \pm 0.3^{a}}$	$\mathbf{0.9 \pm 0.1^{b}}$	$\mathbf{1.8 \pm 0.2^{a}}$	$\mathbf{\chi^2_{(df=6)} = 12.5}$	$\boldsymbol{P = 0.006}$
	Vacuolation of the epithelium	0.8 ± 0.2^{a}	0.4 ± 0.3^{a}	0.6 ± 0.3^{a}	$\chi^2_{(df=6)} = 5.3$	$P = 0.255$
	AGLC (%)	$\mathbf{12.9 \pm 1.6^{a}}$	$\mathbf{6.5 \pm 0.8^{b}}$	$\mathbf{3.6 \pm 0.4^{b}}$	$\mathbf{F_{(df=2)} = 20.3}$	$\boldsymbol{P = 0.000}$
	NGLC (%)	$\mathbf{22.1 \pm 1.6^{a}}$	$\mathbf{9.8 \pm 1.2^{c}}$	$\mathbf{15.4 \pm 1.8^{b}}$	$\mathbf{F_{(df=2)} = 16.3}$	$\boldsymbol{P = 0.000}$
Intestine	Hemocyte infiltration	1.5 ± 0.2^{a}	1.6 ± 0.2^{a}	1.4 ± 0.2^{a}	$\chi^2_{(df=6)} = 2.3$	$P = 0.685$
	Vacuolation of the epithelium	1.1 ± 0.2^{a}	1.4 ± 0.3^{a}	0.8 ± 0.1^{a}	$\chi^2_{(df=6)} = 6.2$	$P = 0.397$
	AGLC (%)	$\mathbf{10.8 \pm 1^{a}}$	$\mathbf{7.8 \pm 1.6^{ab}}$	$\mathbf{4.5 \pm 0.5^{b}}$	$\mathbf{F_{(df=2)} = 8.1}$	$\boldsymbol{P = 0.000}$
	NGLC (%)	$\mathbf{23.6 \pm 2^{a}}$	$\mathbf{15.9 \pm 1.6^{b}}$	$\mathbf{16 \pm 1.8^{b}}$	$\mathbf{F_{(df=2)} = 7.4}$	$\boldsymbol{P = 0.001}$
Digestive gland	Deformation of the epithelium	0.8 ± 0.3^{a}	1.3 ± 0.3^{a}	1.2 ± 0.3^{a}	$\chi^2_{(df=6)} = 3.2$	$P = 0.779$
	AGLC (%)	$\mathbf{31 \pm 2.3^{a}}$	$\mathbf{19 \pm 1.3^{b}}$	$\mathbf{8.2 \pm 0.7^{c}}$	$\mathbf{F_{(df=2)} = 53.3}$	$\boldsymbol{P = 0.000}$
	NGLC (%)	$\mathbf{25.2 \pm 1.4^{a}}$	$\mathbf{4.8 \pm 0.4^{b}}$	$\mathbf{22.2 \pm 1.8^{a}}$	$\mathbf{F_{(df=2)} = 66.6}$	$\boldsymbol{P = 0.000}$

Results are expressed as mean ± SE (*n* = 10 individuals per condition). Data of histopathological observations, and histochemical changes, were analyzed using the experimental condition (three levels) as factor in separate Chi-square test (χ^2) and univariate ANOVA's ($P < 0.05$) respectively. The χ^2 test and the F-test statistic's, as well as the degrees of freedom (df) are reported. Different superscript letters indicate significant differences at $P < 0.05$.

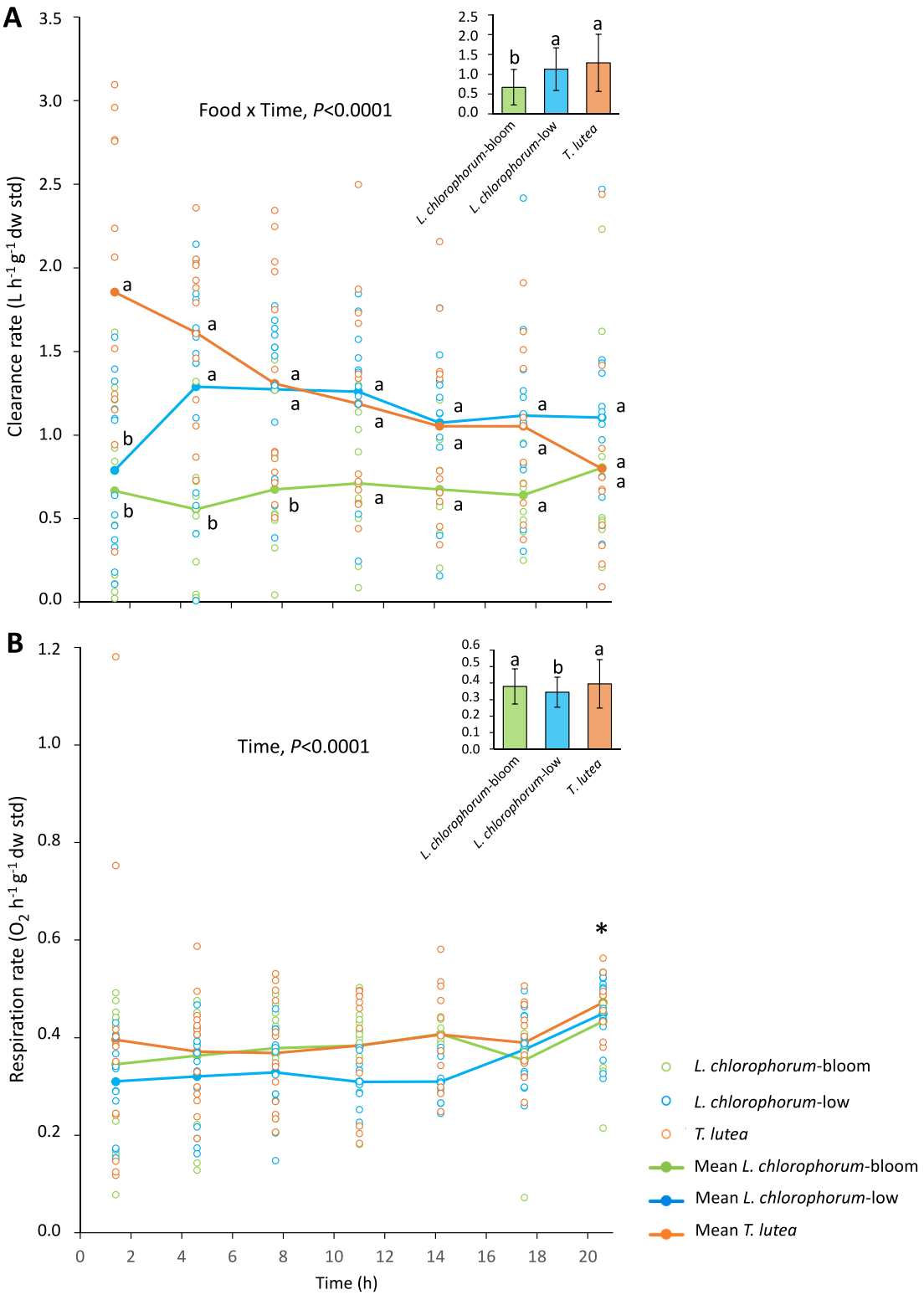

Fig. 5. (A) Individual clearance rate of oysters as a function of food regime and time during the recovery phase: *T. lutea* (orange; $N = 13$), *L. chlorophorum*-low (blue; $N = 13$) and L. *chlorophorum*-bloom (green; $N = 12$). Different superscript letters denote significant differences for the food × time interaction on clearance rate for each time independently (repeated measures ANOVA, $\alpha = 0.05$). The inset shows clearance rate as a function of food regime only. (B) Individual respiration rate of oysters during the recovery phase. * indicate the effect of time on the respiration rate (repeated measures ANOVA, $\alpha = 0.05$). The inset shows respiration rate as a function of food regime only. Open circles represent individuals and solid lines represent mean. (For interpretation of the references to colour in this figure legend, the reader is referred to the web version of this article.)

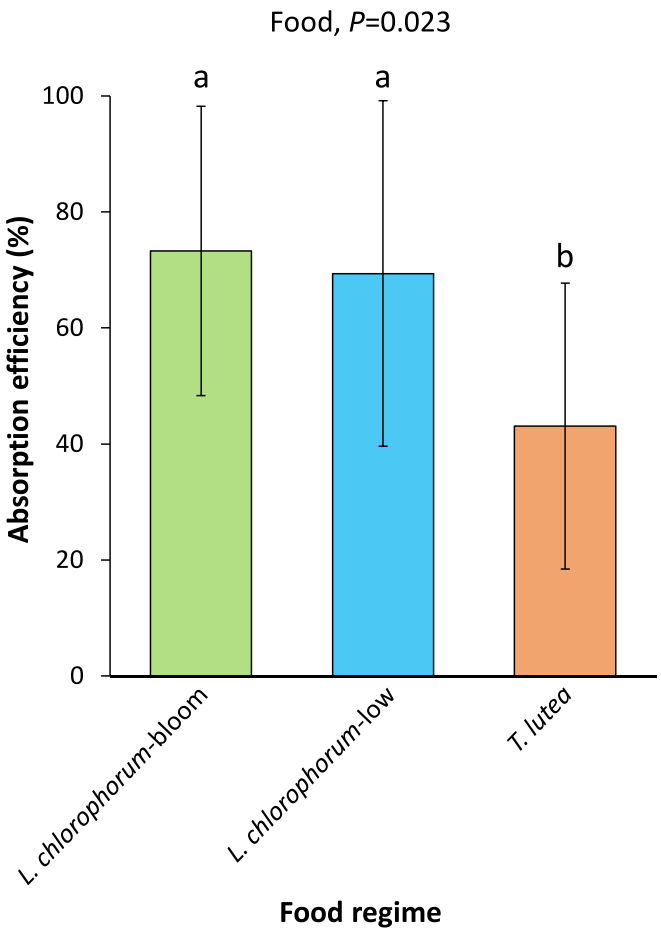

Fig. 6. Absorption Efficiency (%) of oysters as a function of food during the recovery phase: *T. lutea* (N = 13), *L. chlorophorum*-low (N = 13) and *L. chlorophorum*-bloom (N = 12). Data (mean ± SD) were analyzed using the food regime (three levels) as factor in a one-way ANOVA (α = 0.05). Different superscript letters denote statistically significant differences between treatments.

on oyster physiological rates. We expected that oysters exposed to L. *chlorophorum* would reduce their metabolic rates, as usually occurs with poor quality or toxic diet, and thus compensate during the recovery period. It has been reported that the oyster *C. gigas* could reduce clearance, ingestion, and biodeposition rates when exposed to toxic *Alexandrium minutum* (Bougrier et al., 2003; Lassus et al., 2004; Pousse et al., 2018). Here we found that during the 24 h of the recovery phase, the clearance rate measured between 1.4 h and 11 h was significantly higher in the *T. lutea* control condition than in the L. *chlorophorum*-bloom and L. *chlorophorum*-low conditions. The clearance rate of suspension-feeding bivalves has been considered the main responsive component of filter behavior under changing environmental conditions (Hawkins et al., 2001; Cranford et al., 2005; Hégaret et al., 2007; Estrada et al., 2010). During the 48 h exposure phase, oysters in the L. *chlorophorum*-bloom condition were exposed to the highest amounts of TEPs produced by *L. chlorophorum*, which could increase the viscosity of seawater (Kesaulya et al., 2008; Seuront and Vincent, 2008). Modification of seawater viscosity could strongly affect filtration rates in bivalves since it has been shown this controls the cilia beat frequency in *Mytilus edulis* (Riisgård and Larsen, 2007). Although seawater viscosity was not estimated in this work, a new hypothesis suggests that TEPs excreted by L. *chlorophorum* at bloom concentrations could affect the oyster gills through a significant mucus production, resulting in a decreasing clearance rate shortly after exposure to green seawater discolorations.

Previous investigations have shown significant decreases in *C. virginica* clearance rates when fed with high densities of *A. lagunensis*, known to excrete exopolymers and form dense brown tides (Gobler et al., 2013). The authors suggested that pseudo-feces production by the oysters was not enough to compensate for the high seston loads during *A. lagunensis* bloom (Gobler et al., 2013). In the field, Galimany et al. (2017) reported a decrease in clearance rate while absorption efficiency remained constant, suggesting that *C. virginica* was able to sustain its feeding requirements during the brown tides. The stickiness of TEPs could inhibit the activity of cilia and impairs the transport of particles to the mouth (Galimany et al., 2017). Interestingly, oysters previously exposed to L. *chlorophorum* bloom showed a lower clearance rate within the first hours of the short-term recovery experiment, while absorption efficiency was 2-fold higher compared to the control. This increase in food absorption without pseudo-feces production during the recovery phase could suggest a compensation response for a decrease that occurred during the exposure phase.

The exposition of *C. gigas* to L. *chlorophorum* does not appear to strongly affect the individual respiration rate during recovery. Nonetheless, a recent field investigation reported high TEP concentrations during green seawater discolorations, setting hypoxia conditions following this event (Roux et al., 2022). Bacterial remineralization might sustain bloom development for more than one month, causing hypoxia, and likely contributing to bivalve mortality (Roux et al., 2021, 2022). The reduction of feeding activity and oxygen consumption is a common physiological response to hypoxia in marine bivalves (Sobral and Widdows, 1997; Hicks and McMahon, 2002). Therefore, an increase in exposure time would provide further information on the potential effect of L. *chlorophorum* blooms through the hypoxia phenomena and its high production of TEPs.

5. Conclusions

For the first time, our study suggests that the presence of L. *chlorophorum* could significantly affect the ecophysiology of cupped oysters (*e.g.*, inflammatory process in some tissues, low clearance rate measured during the recovery phase, potential altered absorption efficiency).

Indeed, the results allowed us to formulate the new hypothesis that TEPs produced during green seawater discolorations could have a harmful effect on oyster's physiology. This negative effect would have particular relevance during prolonged blooms. The poor food-nutrient storage after the bloom is supported by the previous hypothesis based on the Dynamic Energy Budget model, suggesting that *C. gigas* has a low absorption efficiency for L. *chlorophorum*. Nonetheless, we cannot exclude that hypoxia conditions after a bloom could represent an additional harmful effect on oysters.

Therefore, the overall impairments during L. *chlorophorum* blooms could affect oyster ecophysiology through several mechanisms, such as food-absorption difficulties and clogging of the gills affecting feeding behavior, the subsequent physiological weakening of the poorly nourished animals, making them more sensitive to external hazards (pathogens, pollutants), or, simply by prolonged hypoxia conditions. Further investigations must address the field study of the synergistic effect of longer exposure and higher cell concentrations to confirm these hypotheses since these unfavorable conditions were found as detrimental to oyster's general physiology.

Ethics statement

The juvenile oysters (*Crassostrea gigas*) used in this work were produced and handled according to the International Standards for the Care and Use of Laboratory Animals. The number of sampled organisms contemplated "the rule of maximizing information published and minimizing unnecessary studies". In this sense, 200 oysters were considered as the minimum number of organisms needed for this work.

Funding

This work received financial support from the research project "CLOCLO" (éCophysioLOgie de l'huître creuse exposée à Lepidodinium ChLOrophorum) financed by the IFREMER and Region Pays de la Loire (project LEPIDO-PEN [06582 2019]) under the academic responsibility of RS, MS and EF. PR and JLGC were recipients of doctorate fellowships from IFREMER-Region Pays de la Loire and CONACyT, Mexico (REF: 2019–000025-01EXTF-00067), respectively.

CRediT authorship contribution statement

Pauline Roux: Data curation, Investigation, Writing – original draft, Writing – review & editing, Conceptualization, Methodology. **José Luis García-Corona:** Formal analysis, Validation, Writing – original draft, Methodology, Writing – review & editing. **Stacy Ragueneau:** Formal analysis, Methodology, Writing – original draft. **Mathilde Schapira:** Formal analysis, Funding acquisition, Methodology, Project administration, Writing – review & editing, Supervision, Writing – original draft. **Raffaele Siano:** Data curation, Formal analysis, Methodology, Supervision, Validation, Project administration, Writing – review & editing. **Fabrice Pernet:** Formal analysis, Methodology, Validation. **Isabelle Queau:** Data curation, Formal analysis, Methodology. **Pascale Malestroit:** Data curation, Methodology, Validation. **Kevin Tallec:** Formal analysis, Methodology, Software. **Elodie Fleury:** Conceptualization, Formal analysis, Methodology, Writing – original draft, Writing – review & editing.

Declaration of competing interest

The authors declare that they have no known competing financial interests or personal relationships that could have appeared to influence the work reported in this paper.

Data availability

The evidence and data that support the findings of this study are available from the corresponding author upon reasonable request.

Acknowledgments

The authors are grateful to Marianne Alunno-Bruscia (Ifremer, Brest) for her assistance during the installation of the ecophysiological measurement system, Anne Schmitt (Ifremer, Nantes) for TEP measurements, as well as Claudie Quéré and Valerian Le Roy (Ifremer, Brest) for their technical support with biochemical analysis. We also thank SMIDAP, and especially Philippe Glize for the interest and advice given during the project, and Helene Hegaret (IUEM-LEMAR, Brest) for her assistance with microanatomical observations.

Appendix A. Supplementary data

Supplementary data to this article can be found online at https://doi.org/10.1016/j.aquaculture.2024.740644.

References

Alldredge, A.L., Passow, U., Logan, B.E., 1993. The abundance and significance of a class of large, transparent organic particles in the ocean. Deep-Sea Res. I Oceanogr. Res. Pap. 40 (6), 1131–1140. https://doi.org/10.1016/0967-0637(93)90129-Q.

Alunno-Bruscia, M., Bourlès, Y., Maurer, D., Robert, S., Mazurié, J., Gangnery, A., Goulletquer, P., Pouvreau, S., 2011. A single bioenergetics growth and reproduction model for the oyster *Crassostrea gigas* in six Atlantic ecosystems. J. Sea Res. 66 (4), 340–348. https://doi.org/10.1016/j.seares.2011.07.008.

Barber, B.J., Blake, N.J., 2006. Reproductive physiology. In: Shumway, S.E., Parsons, G. J. (Eds.), Scallops: Biology, Ecology and Aquaculture. Elsevier Science, Boston, MA, pp. 357–406.

Bayne, B., 2002. A physiological comparison between Pacific oysters *Crassostrea gigas* and Sydney Rock oysters *Saccostrea glomerata*: food, feeding and growth in a shared estuarine habitat. Mar. Ecol. Prog. Ser. 232, 163–178. https://doi.org/10.3354/meps232163.

Bayne, B., 2017. Biology of Oysters, , 1st ed.vol. 41. Academic Press, Waltham, MA, pp. 2–844.

Bayne, B., Hawkins, A.J.S., Navarro, E., 1987. Feeding and digestion by the mussel (Bivalvia : Mollusca) in mixtures of silt low concentrations. J. Exp. Mar. Biol. Ecol. 3, 1–22. https://doi.org/10.1016/0022-0981(87)90017-7.

Belin, C., Soudant, D., Amzil, Z., 2021. Three decades of data on phytoplankton and phycotoxins on the French coast: lessons from REPHY and REPHYTOX. Harmful Algae 102, 101733. https://doi.org/10.1016/j.hal.2019.101733.

Beninger, P.G., St-Jean, S., 1997. Particle processing on the labial palps of *Mytilus edulis* and *Placopecten magellanicus* (Mollusca: Bivalvia). Mar. Ecol. Prog. Ser. 147, 117–127. https://doi.org/10.3354/meps147117.

Bougrier, S., Lassus, P., Bardouil, M., Masselin, P., Truquet, P., 2003. Paralytic shellfish poison accumulation yields and feeding time activity in the Pacific oyster *(Crassostrea gigas)* and king scallop *(Pecten maximus)*. Aquat. Living Resour. 16 (4), 347–352. https://doi.org/10.1016/S0990-7440(03)00080-9.

Bourlès, Y., Alunno-Bruscia, M., Pouvreau, S., Tollu, G., Leguay, D., Arnaud, C., Goulletquer, P., Kooijman, S.A.L.M., 2009. Modelling growth and reproduction of the Pacific oyster *Crassostrea gigas*: advances in the oyster-DEB model through application to a coastal pond. J. Sea Res. 62 (2–3), 62–71. https://doi.org/10.1016/j.seares.2009.03.002.

Chapelle, A., Lazure, P., Ménesguen, A., 1994. Modelling eutrophication events in a coastal ecosystem. Sensitivity analysis. Estuar. Coast. Shelf Sci. 39 (6), 529–548. https://doi.org/10.1016/S0272-7714(06)80008-9.

Claquin, P., Probert, I., Lefebvre, S., Veron, B., 2008. Effects of temperature on photosynthetic parameters and TEP production in eight species of marine microalgae. Aquat. Microb. Ecol. 51, 1–11. https://doi.org/10.3354/ame01187.

Conover, R.J., 1966. Assimilation of organic matter by zooplankton. Limnol. Oceanogr. 11 (3), 338–345. https://doi.org/10.4319/lo.1966.11.3.0338.

Costa, P., Costa, M.H., 2012. Development and application of a novel histological multichrome technique for clam histopathology. J. Invertebr. Pathol. 110, 411–414. https://doi.org/10.1016/j.jip.2012.04.013.

Cranford, P.J., Armsworthy, S.L., Mikkelsen, O.A., Milligan, T.G., 2005. Food acquisition responses of the suspension-feeding bivalve *Placopecten magellanicus* to the flocculation and settlement of a phytoplankton bloom. J. Exp. Mar. Biol. Ecol. 326 (2), 128–143. https://doi.org/10.1016/j.jembe.2005.05.012.

Delaporte, M., Soudant, P., Lambert, C., Moal, J., Pouvreau, S., Samain, J.F., 2006. Impact of food availability on energy storage and defense related hemocyte parameters of the Pacific oyster *Crassostrea gigas* during an experimental reproductive cycle. Aquaculture. 254 (1–4), 571–582. https://doi.org/10.1016/j.aquaculture.2005.10.006.

Díaz, A.O., García, A.M., Goldemberg, A.L., 2008. Glycoconjugates in the mucosa of the digestive tract of *Cynoscion guatucupa*: a histochemical study. Acta Histochem. 110 (1), 76–85. https://doi.org/10.1016/j.acthis.2007.08.002.

Dupuy, C., Vaquer, A., Lam-Hôai, T., Rougier, C., Mazouni, N., Lautier, J., Collos, Y., Le Gall, S., 2000. Feeding rate of the oyster *Crassostrea gigas* in a natural planktonic community of the Mediterranean Thau Lagoon. Mar. Ecol. Prog. Ser. 205, 171–184. https://www.jstor.org/stable/24863659.

Elbrächter, M., Schnepf, E., 1996. *Gymnodinium chlorophorum*, a new, green, bloom-forming dinoflagellate (Gymnodiniales, Dinophyceae) with a vestigial prasinophyte endosymbiont. Phycologia. 35 (5), 381–393. https://doi.org/10.2216/i0031-8884-35-5-381.1.

Estrada, N., Rodríguez-Jaramillo, C., Contreras, G., Ascencio, F., 2010. Effects of induced paralysis on hemocytes and tissues of the giant lions-paw scallop by paralyzing shellfish poison. Mar. Biol. 157 (6), 1401–1415. https://doi.org/10.1007/s00227-010-1418-4.

Fabioux, C., Huvet, A., Le Souchu, P., Le Pennec, M., Pouvreau, S., 2005. Temperature and photoperiod drive *Crassostrea gigas* reproductive internal clock. Aquaculture. 250 (1–2), 458–470. https://doi.org/10.1016/j.aquaculture.2005.02.038.

Gabbott, P.A., 1975. Storage cycles in marine bivalve mollusks: A hypothesis concerning the relationship between glycogen metabolism and gametogenesis. In: Barnes, H. (Ed.), Proceedings of the 9th European Marine Biology Symposium. Aberdeen University Press, Aberdeen, pp. 191–211.

Galimany, E., Lunt, J., Freeman, C.J., Reed, S., Segura-García, I., Paul, V.J., 2017. Feeding behavior of eastern oysters *Crassostrea virginica* and hard clams *Mercenaria mercenaria* in shallow estuaries. Mar. Ecol. Prog. Ser. 567, 125–137. https://doi.org/10.3354/meps12050.

Gao, X., Mu, C., Li, Q., 2021. Effects of toxic dinoflagellate *Alexandrium catenella* on sexual maturation and reproductive output in the pacific oyster *Crassostrea gigas*. Aquat. Toxicol. 232, 105745 https://doi.org/10.1016/j.aquatox.2021.105745.

Gárate-Lizárraga, I., Muñetón-Gómez, M.S., Pérez-Cruz, B., Díaz-Ortíz, J.A., 2014. Bloom of *Gonyaulax spinifera* (Dinophyceae: Gonyaulacales) in ensenada de la Paz Lagoon, Gulf of California. CICIMAR Oceánides 29 (1), 11–18. https://doi.org/10.37543/oceanides.v29i1.130.

García-Corona, J.L., Rodríguez-Jaramillo, C., Saucedo, P.E., López-Carvallo, J.A., Arcos-Ortega, G.F., Mazón-Suástegui, J.M., 2018. Internal energy management associated with seasonal gonad development and oocyte quality in the Horsemussel *Modiolus capax* (Bivalvia; Mytilidae). J. Shellfish Res. 37 (3), 475–483. https://doi.org/10.2983/035.037.0302.

García-Corona, J.L., Hegaret, H., Deléglise, M., Marzari, A., Rodríguez-Jaramillo, C., Foulon, V., Fabioux, C., 2022. First subcellular localization of the amnesic shellfish toxin, domoic acid, in bivalve tissues: deciphering the physiological mechanisms

involved in its long-retention in the king scallop *Pecten maximus*. Harmful Algae 116, 102251. https://doi.org/10.1016/j.hal.2022.102251.
García-Oliva, O., Hantzsche, F.M., Boersma, M., Wirtz, K.W., 2022. Phytoplankton and particle size spectra indicate intense mixotrophic dinoflagellates grazing from summer to winter. J. Plankton Res. 44 (2), 224–240. https://doi.org/10.1093/plankt/fbac013.
Ghosh, S., 2020. Sialic Acids and Sialoglycoconjugates in the Biology of Life, Health and Disease, 1st ed. Academic Press.
Gobler, C.J., Berry, D.L., Anderson, O.R., Burson, A., Koch, F., Rodgers, B.S., Moore, L.K., Goleski, J.A., Allam, B., Bowser, P., Tang, Y., Nuzzi, R., 2008. Characterization, dynamics, and ecological impacts of harmful *Cochlodinium polykrikoides* blooms on eastern Long Island, NY, USA. Harmful Algae 7 (3), 293–307. https://doi.org/10.1016/j.hal.2007.12.006.
Gobler, C.J., Koch, F., Kang, Y., Berry, D.L., Tang, Y.Z., Lasi, M., Walters, L., Hall, L., Miller, J.D., 2013. Expansion of harmful brown tides caused by the pelagophyte, *Aureoumbra lagunensis* DeYoe et Stockwell, to the US east coast. Harmful Algae 27, 29–41. https://doi.org/10.1016/j.hal.2013.04.004.
Guillard, R., Hargraves, P., 1993. *Stichochrysis immobilis* is a diatom, not a chrysophyte. Phycologia. 32, 234–236. https://doi.org/10.2216/i0031-8884-32-3-234.1.
Haberkorn, H., Lambert, C., Le Goïc, N., Moal, J., Suquet, M., Guéguen, M., Sunila, I., Soudant, P., 2010. Effects of *Alexandrium minutum* exposure on nutrition-related processes and reproductive output in oysters *Crassostrea gigas*. Harmful Algae 9 (5), 427–439. https://doi.org/10.1016/j.hal.2010.01.003.
Hansen, G., Botes, L., de Salas, M., 2007. Ultrastructure and large subunit rDNA sequences of *Lepidodinium viride* reveal a close relationship to *Lepidodinium chlorophorum* comb. nov. (= *Gymnodinium chlorophorum*). Phycol. Res. 55 (1), 25–41. https://doi.org/10.1111/j.1440-1835.2006.00442.x.
Hawkins, A.J.S., Fang, J.G., Pascoe, P.L., Zhang, J.H., Zhang, X.L., Zhu, M.Y., 2001. Modelling short-term responsive adjustments in particle clearance rate among bivalve suspension-feeders: separate unimodal effects of seston volume and composition in the scallop *Chlamys farreri*. J. Exp. Mar. Biol. Ecol. 262 (1), 61–73. https://doi.org/10.1016/S0022-0981(01)00282-9.
Hector, A., 2015. The New Statistics with R: An Introduction for Biologists, 1st ed. Oxford University Press, New York.
Hégaret, H., Wikfors, G.H., Shumway, S.E., 2007. Diverse feeding responses of five species of bivalves mollusc when exposed to three species of harmful algae. J. Shellfish Res. 26 (2), 549–559. https://doi.org/10.2983/0730-8000(2007)26[549:DFROFS]2.0.CO;2.
Hégaret, H., Smolowitz, R.M., Sunila, I., Shumway, S.E., Alix, J., Dixon, M., Wikfors, G. H., 2010. Combined effects of a parasite, QPX, and the harmful-alga, *Prorocentrum minimum* on northern quahogs, *Mercenaria mercenaria*. Mar. Environ. Res. 69 (5), 337–344. https://doi.org/10.1016/j.marenvres.2009.12.008.
Hégaret, H., Brokordt, K.B., Gaymer, C.F., Lohrmann, K.B., García, C., Varela, D., 2012. Effects of the toxic dinoflagellate *Alexandrium catenella* on histopathogical and escape responses of the Northern scallop *Argopecten purpuratus*. Harmful Algae 18, 74–83. https://doi.org/10.1016/j.hal.2012.04.006.
Hicks, D.W., McMahon, R.F., 2002. Respiratory responses to temperature and hypoxia in the nonindigenous Brown Mussel, *Perna perna* (Bivalvia: Mytilidae), from the Gulf of Mexico. J. Exp. Mar. Biol. Ecol. 277 (1), 61–78. https://doi.org/10.1016/S0022-0981(02)00276-9.
Iglesias, J.I.P., Urrutia, M.B., Navarro, E., Ibarrola, I., 1998. Measuring feeding and absorption in suspension-feeding bivalves: an appraisal of the biodeposition method. J. Exp. Mar. Biol. Ecol. 219 (1–2), 71–86. https://doi.org/10.1016/S0022-0981(97)00175-5.
Izzetoğlu, S., Şahar, U., Şener, E., Deveci, R., 2014. Determination of sialic acids in immune system cells (coelomocytes) of sea urchin, *Paracentrotus lividus*, using capillary LC-ESI-MS/MS. Fish Shellfish Immunol. 36 (1), 181–186. https://doi.org/10.1016/j.fsi.2013.10.029.
Kesaulya, I., Leterme, S.C., Mitchell, J.G., Seuront, L., 2008. The impact of turbulence and phytoplankton dynamics on foam formation, seawater viscosity and chlorophyll concentration in the eastern English Channel. Oceanologia. 50 (2), 167–182.
Kim, Y., Ashton-Alcox, K.A., Powell, E.N., 2006. Histological Techniques for Marine Bivalve Molluscs: Update. NOAA Technical Memorandum NOS NCCOS 27, Maryland.
Kromkamp, J.C., Forster, R.M., 2003. The use of variable fluorescence measurements in aquatic ecosystems: differences between multiple and single turnover measuring protocols and suggested terminology. Eur. J. Phycol. 38 (2), 103–112. https://doi.org/10.1080/0967026031000094094.
Lassudrie, M., Soudant, P., Richard, G., Henry, N., Medhioub, W., da Silva, P.M., Donval, A., Bunel, M., Le Goïc, N., Lambert, C., de Montaudouin, X., Fabioux, C., Hégaret, H., 2014. Physiological responses of Manila clams *Venerupis* (=*Ruditapes*) *philippinarum* with varying parasite *Perkinsus olseni* burden to toxic algal *Alexandrium ostenfeldii* exposure. Aquat. Toxicol. 154, 27–38. https://doi.org/10.1016/j.aquatox.2014.05.002.
Lassudrie, M., Hégaret, H., Wikfors, G.H., da Silva, P.M., 2020. Effects of marine harmful algal blooms on bivalve cellular immunity and infectious diseases: a review. Dev. Comp. Immunol. 108 (103660) https://doi.org/10.1016/j.dci.2020.103660.
Lassus, P., Baron, R., Garen, P., Truquet, P., Masselin, P., Bardouil, M., Leguay, D., Amzil, Z., 2004. Paralytic shellfish poison outbreaks in the Penzé estuary: environmental factors affecting toxin uptake in the oyster, *Crassostrea gigas*. Aquat. Living Resour. 17 (2), 207–214. https://doi.org/10.1051/alr:2004012.
Li, B., Ward, J.E., Holohan, B.A., 2008. Transparent exopolymer particles (TEP) from marine suspension feeders enhance particle aggregation. Mar. Ecol. Prog. Ser. 357, 67–77. https://doi.org/10.3354/meps07290.
López-Carvallo, J.A., Saucedo, P.E., Rodríguez-Jaramillo, C., Campa-Córdova, A.I., García-Corona, J.L., Mazón-Suástegui, J.M., 2017. Carbohydrate-rich diets meet energy demands of gametogenesis in hatchery-conditioned *Modiolus capax* mussels at increasing temperatures. J. Shellfish Res. 36, 649–657. https://doi.org/10.2983/035.036.0314.
Martins, E., Figueras, A., Novoa, B., Santos, R.S., Moreira, R., Bettencourt, R., 2014. Comparative study of immune responses in the deep-sea hydrothermal vent mussel *Bathymodiolus azoricus* and the shallow-water mussel *Mytilus galloprovincialis* challenged with *Vibrio* bacteria. Fish Shellfish Immunol. 40 (2), 485–499. https://doi.org/10.1016/j.fsi.2014.07.018.
McCarthy, P.M., 2013. Census of Australian Marine Dinofagellates. Australian Biological Resources Study, Canberra. http://www.anbg.gov.au/abrs/Dinoflagellates/index_Dino.html. Accessed 24 Febuary 2022.
McKee, M.P., Ward, J.E., MacDonald, B.A., Holohan, B.A., 2005. Production of transparent exopolymer particles (TEP) by the eastern oyster *Crassostrea virginica*. Mar. Ecol. Prog. Ser. 288, 141–149. https://doi.org/10.3354/meps288141.
Medhioub, W., Lassus, P., Truquet, P., Bardouil, M., Amzil, Z., Sechet, V., Sibat, M., Soudant, P., 2012. Spirolide uptake and detoxification by *Crassostrea gigas* exposed to the toxic dinoflagellate *Alexandrium ostenfeldii*. Aquaculture. 358–359, 108–115. https://doi.org/10.1016/j.aquaculture.2012.06.023.
Neves, R.A.F., Santiago, T.C., Carvalho, W.F., dos Silva, E.S., da Silva, P.M., Nascimento, S.M., 2019. Impacts of the toxic benthic dinoflagellate *Prorocentrum lima* on the brown mussel *Perna perna*: Shell-valve closure response, immunology, and histopathology. Mar. Environ. Res. 146, 35–45. https://doi.org/10.1016/j.marenvres.2019.03.006.
Passow, U., Alldredge, A.L., 1995. A dye-binding assay for the spectrophotometric measurement of transparent exopolymer particles (TEP). Limnol. Oceanogr. 40 (7), 1326–1335. https://doi.org/10.4319/lo.1995.40.7.1326.
Passow, U., Shipe, R.F., Murray, A., Pak, D.K., Brzezinski, M.A., Alldredge, A.L., 2001. The origin of transparent exopolymer particles (TEP) and their role in the sedimentation of particulate matter. Cont. Shelf Res. 21 (4), 327–346. https://doi.org/10.1016/S0278-4343(00)00101-1.
Pernet, F., Malet, N., Pastoureaud, A., Vaquer, A., Quéré, C., Dubroca, L., 2012. Marine diatoms sustain growth of bivalves in a Mediterranean lagoon. J. Sea Res. 68, 20–32. https://doi.org/10.1016/j.seares.2011.11.004.
Petton, B., Bruto, M., James, A., Labreuche, Y., Alunno-Bruscia, M., Le Roux, F., 2015. *Crassostrea gigas* mortality in France: the usual suspect, a herpes virus, may not be the killer in this polymicrobial opportunistic disease. Front. Microbiol. 6, 686. https://doi.org/10.3389/fmicb.2015.00686.
Pousse, É., Flye-Sainte-Marie, J., Alunno-Bruscia, M., Hégaret, H., Jean, F., 2018. Sources of paralytic shellfish toxin accumulation variability in the Pacific oyster *Crassostrea gigas*. Toxicon. 144, 14–22. https://doi.org/10.1016/j.toxicon.2017.12.050.
Pouvreau, S., Bourles, Y., Lefebvre, S., Gangnery, A., Alunno-Bruscia, M., 2006. Application of a dynamic energy budget model to the Pacific oyster, *Crassostrea gigas*, reared under various environmental conditions. J. Sea Res. 56 (2), 156–167. https://doi.org/10.1016/j.seares.2006.03.007.
R Core Team, 2020. R: A Language and Environment for Statistical Computing. R Foundation for Statistical Computing, Vienna, Austria. URL. https://www.R-project.org/.
Riisgård, H.U., Larsen, P.S., 2007. Viscosity of seawater controls beat frequency of water-pumping cilia and filtration rate of mussels *Mytilus edulis*. Mar. Ecol. Prog. Ser. 343, 141–150. https://doi.org/10.3354/meps06930.
Rodríguez-Benito, C.V., Navarro, G., Caballero, I., 2020. Using Copernicus Sentinel-2 and Sentinel-3 data to monitor harmful algal blooms in southern Chile during the COVID-19 lockdown. Mar. Pollut. Bull. 161, 111722 https://doi.org/10.1016/j.marpolbul.2020.111722.
Rodríguez-Jaramillo, C., Hurtado, M.A., Romero-Vivas, E., Ramírez, E., Manzano, M., Palacios, E., 2008. Gonadal development and histochemestry of the tropical oyster, *Crassostrea corteziensis* (Hertlein, 1951) during an annual reproductive cycle. J. Shellfish Res. 27, 1129–1141. https://doi.org/10.2983/0730-8000-27.5.1129.
Rodríguez-Jaramillo, C., García-Corona, J.L., Zenteno-Savín, T., Palacios, E., 2022. The effects of experimental temperature increase on gametogenesis and heat stress parameters in oysters: comparison of a temperate-introduced species (*Crassostrea gigas*) and a native tropical species (*Crassostrea corteziensis*). Aquaculture. 561, 738683 https://doi.org/10.1016/j.aquaculture.2022.738683.
Roux, P., Siano, R., Collin, K., Bilien, G., Sinquin, C., Marchand, L., Zykwinska, A., Delbarre-Ladrat, C., Schapira, M., 2021. Bacteria enhance the production of extracellular polymeric substances by the green dinoflagellate *Lepidodinium chlorophorum*. Sci. Rep. 11 (1), 4795. https://doi.org/10.1038/s41598-021-84253-2.
Roux, P., Siano, R., Souchu, P., Collin, K., Schmitt, A., Manach, S., Retho, M., Pierre-Duplessix, O., Marchand, L., Colliec-Jouault, S., Pochic, V., Zoffoli, M.L., Gernez, P., Schapira, M., 2022. Spatio-temporal dynamics and biogeochemical properties of green seawater discolorations caused by the marine dinoflagellate *Lepidodinium chlorophorum*. Estuar. Coast. Shelf Sci. 275, 107950 https://doi.org/10.1016/j.ecss.2022.107950.
Roux, P., Schapira, M., Mertens, K., André, C., Terre-Terrillon, A., Schmitt, A., Manach, S., Collin, K., Serghine, J., Noel, C., Siano, R., 2023. When phytoplankton do not bloom: the case of the dinoflagellate *Lepidodinium chlorophorum* in southern Brittany (France) assessed by environmental DNA. Prog. Oceanogr. 212, 102999 https://doi.org/10.1016/j.pocean.2023.102999.
Savina, M., Pouvreau, S.A., 2004. Comparative ecophysiological study of two infaunal filter-feeding bivalves: *Paphia rhomboïdes* and *Glycymeris glycymeris*. Aquaculture. 239 (1–4), 289–306. https://doi.org/10.1016/j.aquaculture.2004.05.029.
Serre-Fredj, L., Jacqueline, F., Navon, M., Izabel, G., Chasselin, L., Jolly, O., Repecaud, M., Claquin, P., 2021. Coupling high frequency monitoring and bioassay experiments to investigate a harmful algal bloom in the bay of seine (French-English Channel). Mar. Pollut. Bull. 168, 112387 https://doi.org/10.1016/j.marpolbul.2021.112387.

Seuront, L., Vincent, D., 2008. Increased seawater viscosity, *Phaeocystis globosa* spring bloom and *Temora longicornis* feeding and swimming behaviours. Mar. Ecol. Prog. Ser. 363, 131–145. https://doi.org/10.3354/meps07373.

Siano, R., Chapelle, A., Antoine, V., Michel-Guillou, E., Rigaut-Jalabert, F., Guillou, L., Hégaret, H., Leynaert, A., Curd, A., 2020. Citizen participation in monitoring phytoplankton seawater discolorations. Mar. Policy 117, 103039. https://doi.org/10.1016/j.marpol.2018.01.022.

Sobral, P., Widdows, J., 1997. Influence of hypoxia and anoxia on the physiological responses of the clam *Ruditapes decussatus* from southern Portugal. Mar. Biol. 127, 455–461. https://doi.org/10.1007/s002270050033.

Sourisseau, M., Jegou, K., Lunven, M., Quere, J., Gohin, F., Bryere, P., 2016. Distribution and dynamics of two species of Dinophyceae producing high biomass blooms over the French Atlantic Shelf. Harmful Algae 53, 53–63. https://doi.org/10.1016/j.hal.2015.11.016.

Sournia, A., Belin, C., Billard, C., Erard-Le Denn, E., Fresnel, J., Lassus, P., Pastoureaud, A., Soulard, R., 1992. The repetitive and expanding occurrence of green, bloom-forming dinoflagellate (Dinophyceae) on the coasts of France. Cryptogam. Algol. 13 (1), 1–13. https://archimer.ifremer.fr/doc/00133/24470/.

Tallec, K., Paul-Pont, I., Petton, B., Alunno-Bruscia, M., Bourdon, C., Bernardini, I., Boulais, M., Lambert, C., Quere, C., Bideau, A., Le Goïc, N., Cassone, A.L., Le Grand, F., Fabioux, C., Soudant, P., Huvet, A., 2021. Amino-nanopolystyrene exposures of oyster (*Crassostrea gigas*) embryos induced no apparent intergenerational effects. Nanotoxicology. 15 (4), 477–493. https://doi.org/10.1080/17435390.2021.1879963.

Thomas, Y., Pouvreau, S., Alunno-Bruscia, M., Barillé, L., Gohin, F., Bryère, P., Gernez, P., 2016. Global change and climate-driven invasion of the Pacific oyster (*Crassostrea gigas*) along European coasts: a bioenergetics modelling approach. J. Biogeogr. 43 (3), 568–579. https://doi.org/10.1111/jbi.12665.

Walne, P.R., 1970. Studies on the food value of nineteen genera of algae to juvenile bivalves of the genera *Ostrea, Crassostrea, Mercenaria* and *Mytilus*. Fish. Invest. Lond. 1970 (26), 1–62.

Zar, J.H., 2010. Biostatistical Analysis, 5th ed. Pearson, Westlake Village, CA. 251 pp.